ELSEVIER

Thermochimica Acta 285 (1996) 361–382

thermochimica acta

Reduction of tungsten oxides with hydrogen and with hydrogen and carbon

Dean S. Venables, Michael E. Brown*

Chemistry Department, Rhodes University, Grahamstown, 6140, South Africa

Received 14 November 1995; accepted 27 February 1996

Abstract

The reductions of WO_3 and of WO_3–graphite mixtures with hydrogen were studied in isothermal experiments in a tube furnace from 575 to 975°C, using evolved gas analysis, X-ray powder diffraction, and scanning electron microscopy. The intermediate phases $W_{20}O_{58}$, $W_{18}O_{49}$, and WO_2 were observed in the reductions. The final product of the reductions with hydrogen and carbon was tungsten. The reactant/product gas ratio had a considerable influence on the reactions occurring. The morphology of the sample was characterised at different stages of the reduction. Some particle growth was observed in the reduction with hydrogen and was attributed to the formation of $WO_2(OH)_2(g)$, but the sizes and shapes of the tungsten particles produced were not greatly affected by the presence of carbon.

The reactions were controlled by mass-transfer under the conditions investigated. The addition of carbon increased the rate of the reduction process, but did not affect the phases formed in the system. CO_2 was evolved mainly at the start, and CO mainly at the end of the process. The reaction mechanisms were determined on the basis of the evolved gas analyses.

Results are compared with results obtained in other studies of the reduction using carbon alone and carbon monoxide.

Keywords: Carbothermic; Reduction; Tungsten carbide; Tungsten metal; Tungsten oxides

1. Introduction

Tungsten carbide is produced by carburising tungsten powder with either methane or carbon in the presence of hydrogen gas [1]. Growth of tungsten particles occurs during reduction in hydrogen, thus decreasing the commerical value of the resulting tungsten powder. Water vapour produced by the reduction is responsible for the

* Corresponding author.

PII: S0040-6031(96)02951-6

increase in particle size, because the formation of volatile $WO_2(OH)_2$[2] permits transport of tungsten through the gas phase [3,4]. Reduction using carbon alone may introduce impurities and produces coarse tungsten particles [1]. Reduction of cobalt–tungsten oxides with hydrogen is reported [5] to be improved in the presence of solid carbon. Carbon, by decreasing the concentration of water vapour in the system, forming CO and H_2, should improve the properties of the resulting tungsten and tungsten carbide powders.

This paper deals with the kinetics of reduction of tungsten oxides by hydrogen alone, and by hydrogen and carbon simultaneously. The reductions of tungsten oxides by carbon [6,7] and by carbon monoxide [8] have also been studied.

2. Experimental

2.1. Materials

Were as before [6,7], namely: WO_3 (98% pure, Saarchem, 53–75 μm mesh); graphite (< 53 μm mesh) and lamp black (both 99% pure, Saarchem); WO_2 was prepared by reducing WO_3 at 800°C under hydrogen which had been bubbled through water. $W_{18}O_{49}$ was prepared in a similar manner at 700°C. High purity argon and hydrogen were supplied by Fedgas. Both gases contained less than 3.0 vpm O_2 and 2.0 vpm H_2O. Weighed samples of tungsten oxides and graphite or lamp black were mixed by tumbling for 18 h.

2.2. Tube furnace and gas detection system

Reactions of samples (0.25 to 5.0 g) were studied in a Carbolite MTF 12/38B tube furnace, which had a maximum temperature of 1200°C. The weighed samples were placed in a procelain boat at a fixed position in a stainless-steel reaction tube, which was positioned in the furnace and connected to the gas supply. The temperature in the reaction tube was approximately constant (± 5°C) at the position of the sample. Flexible tubing on both sides of the reaction tube allowed the tube to be inserted into or removed from the furnace.

The exhaust gas from the reaction tube passed through a filter and a digital flowmeter and then, via a heated line, to a Servomex MK158 thermal conductivity detector (TCD) maintained at 150°C. After the TCD, the sample gas passed through separate infrared CO_2 and CO detectors (Edinburgh Sensors).

2.3. Other techniques

The sizes and morphologies of the reactant and product powders were studied using a Jeol JSM-840 scanning electron microscope. A Phillips X-ray diffractometer was used to record the powder diffraction patterns of samples withdrawn from the furnace at various stages of the reduction.

3. Results

3.1. Reduction of tungsten oxides with hydrogen

Samples of WO_3 (1.2 to 1.3 g) were reduced in the tube furnace in hydrogen at different temperatures and flowrates. The product of the reduction was identified as α-W by XRD. The mass losses at the end of the reduction process ranged from 20.7 to 21.4%, which is close to the expected mass loss of 20.70% for the reduction of WO_3 to tungsten metal.

The TCD traces of the reduction of WO_3 at different temperatures and in hydrogen flowing at 200 ml min^{-1} are shown in Figs. 1 and 2 and indicate the sequential nature of the reduction. Four parts of the TCD profile were identified: two small peaks at the start of the reaction, a large peak indicating a high rate of reaction, and finally a considerably slower reaction. At high temperatures, the first and second stages are not readily distinguishable from the third peak, and the fourth stage also increases in rate relative to the preceding stages of the reaction (Table 1).

The composition of the sample was examined at different stages of the process at 675 and 875°C. The results are shown in Table 2. When no more than two phases were present, the approximate composition was calculated. The reaction scheme inferred from these results is:

$$WO_3 \xrightarrow{(1)} W_{20}O_{58} \xrightarrow{(2)} W_{18}O_{49} \xrightarrow{(3)} WO_2 \xrightarrow{(4)} \alpha\text{-W}$$

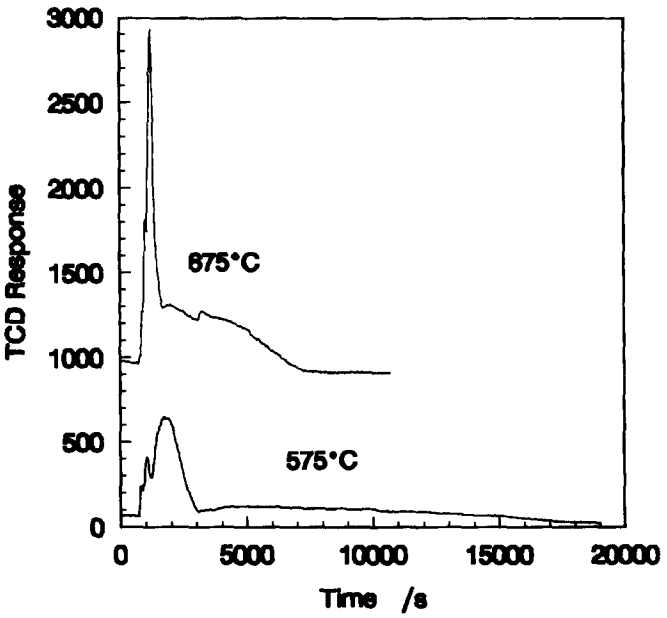

Fig. 1. TCD traces of the isothermal reduction of WO_3 at 575 amd 675 °C in hydrogen flowing at 200 mL min^{-1}.

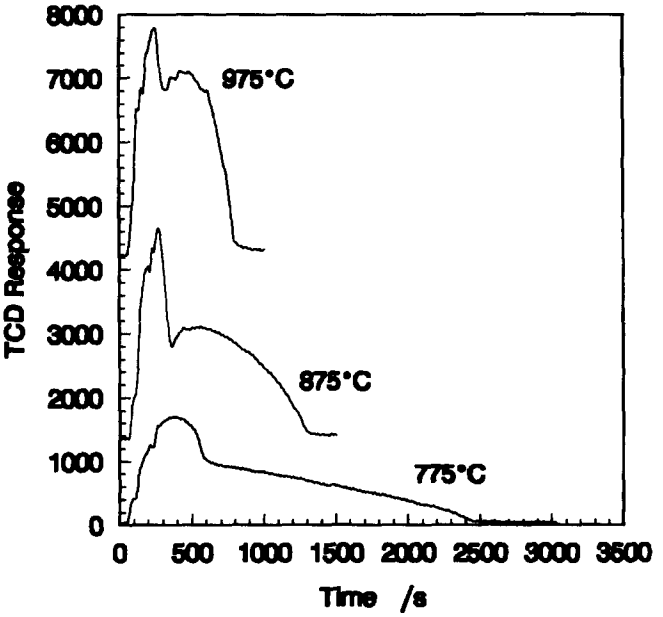

Fig. 2. TCD traces of the isothermal reduction of WO_3 at 775, 875 and 975°C in hydrogen flowing at 200 mL min^{-1}.

Table 1
The durations of the first three stages of the reduction of WO_3 with hydrogen, the fourth stage of reaction, and the total reaction. The ratio of the duration of the first three stages to the fourth stage of reaction is also shown. The hydrogen flow-rate was 200 mL min^{-1}

Temp/°C	Duration of stage			
	Stages 1 to 3/s	Stage 4/s	Complete reaction/s	Time ratio 4/(1 to 3)
575	2380	Incomplete	Incomplete	–
675	960	7140	8100	7.4
775	540	1860	2400	3.4
	450	1730	2180	3.8
875	290	940	1230	3.2
975	250	490	740	2.0

and is very similar to the reaction schemes for the reductions with CO and with solid carbon [6–8]. Not all of the phases and reactions reported by Schubert [9] were identified in this study, most notably the direct reduction of $W_{18}O_{49}$ to tungsten metal. β-W was only identified in trace amounts at 575°C.

The number of steps in the reaction and the amount of oxygen removed in each step suggest that the four parts of the TCD trace may be identified with each of the steps in the scheme above. Samples withdrawn from the furnace at the end of the third stage at

Table 2
The composition of the sample at different times in the reduction of WO_3 with hydrogen at 675°C and at 875°C

Time/min	Mass loss/%	Phase identified and approximate composition
675°C		
5	2.35	80% $W_{18}O_{49}$; 20% $W_{20}O_{58}$
12	8.50	90% WO_2; 10% α-W
40	13.97	50% α-W; 50% WO_2
875°C		
1.5	1.34	$W_{20}O_{58}$
2.5	3.73	80% $W_{18}O_{49}$; 20% WO_2
3.5	5.49	60% WO_2; 40% $W_{18}O_{49}$
5	8.44	90% WO_2; 10% α-W
8	11.81	70% WO_2; 30% α-W
12	17.12	70% α-W; 30% WO_2
16	20.09	90% α-W; 10%WO_2

575 to 975°C all consisted predominantly of WO_2. α-W was the only other phase present, but usually in small quantitites. Thus, the fourth stage in the TCD trace can be identified with the reduction of WO_2 to α-W. From the approximate positions on the TCD traces, the first three peaks in the TCD trace may be similarly associated with reactions (1), (2) and (3) in the scheme above. The relative areas of the peaks at 675 and 875°C were estimated by simple vertical projection and corresponded quite closely with the proportion of the overall reaction of each of the reactions in the reduction, Table 3.

Experiments were conducted in which the hydrogen flow-rate was varied. Fig. 3 shows the durations of the first to third stages, and of the fourth stage of the process at 675, 875 and 975°C. The flow-rate has a marked influence on the reaction rate and this influence increases as the temperature in the system is lowered.

Table 3
Relative areas of the peaks under the TCD traces at 675 and at 875°C for the reduction of WO_3 with hydrogen, compared with the proportion of the overall process of each of the four reactions in the reaction scheme: $WO_3 \xrightarrow{(1)} W_{20}O_{58} \xrightarrow{(2)} W_{18}O_{49} \xrightarrow{(3)} WO_2 \xrightarrow{(4)} \alpha\text{-W}$

Stage of reaction	Relative area of peak/%		
	675°C	875°C	Calculated
First	1.2	1.2	3.3
Second	4.7	11	5.9
Third	31	23	24
Fourth	63	65	67

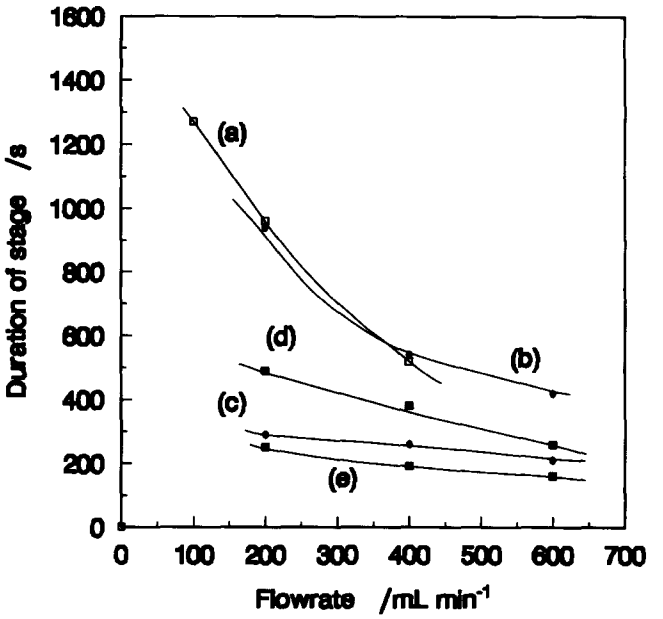

Fig. 3. Effect of the flow-rate on the duration of the reduction of WO_3 with hydrogen: (a) stages 1 to 3 and (b) stage 4, at 675°C; (c) stages 1 to 3 and (d) stage 4, at 875°C; (e) stages 1 to 3 at 975°C.

The H_2/H_2O equilibrium ratios for each of the four steps in the reaction (Fig. 4) provide an explanation of the effect of the flow-rate on the system. The H_2/H_2O equilibrium ratios for the first and second stages of the reduction are less than 0.01 at all the temperatures considered in this study. The flow-rate is thus unlikely to influence these reactions. The equilibrium H_2/H_2O ratio for the reduction of $W_{18}O_{49}$ to WO_2 is, however, larger (Fig. 4, curve (b)) and increases as the temperature is lowered. This accounts for the greater effect of the flow-rate on the reduction at lower temperatures.

The temperature has an even larger bearing on the value of the H_2/H_2O equilibrium ratio for the reduction of WO_2 to tungsten. An increasingly reducing atmosphere is required for the reduction to proceed as the temperature in the system is lowered. The reduction of WO_2 thus becomes more dependent on the flow-rate at low temperatures. The variation of the equilibrium ratios of the four reactions with temperature also explains the observed increase in the duration of the fourth stage, at lower temperatures, relative to the precceding three stages (Table 1).

In gas–solid reactions, the rate of reaction is usually less influenced by the flow-rate at lower temperatures, since the ratio of reactant to product gases in the system decreases relative to the equilibrium concentration and mass-transfer becomes less important. The kinetic parameters of the reaction are therefore often obtained by decreasing the temperature until the reaction is no longer controlled by mass-transfer [10]. In the present system, though, the large increase in the H_2/H_2O ratio required to bring about reduction at low temperatures opposes the decrease in the reduction rate

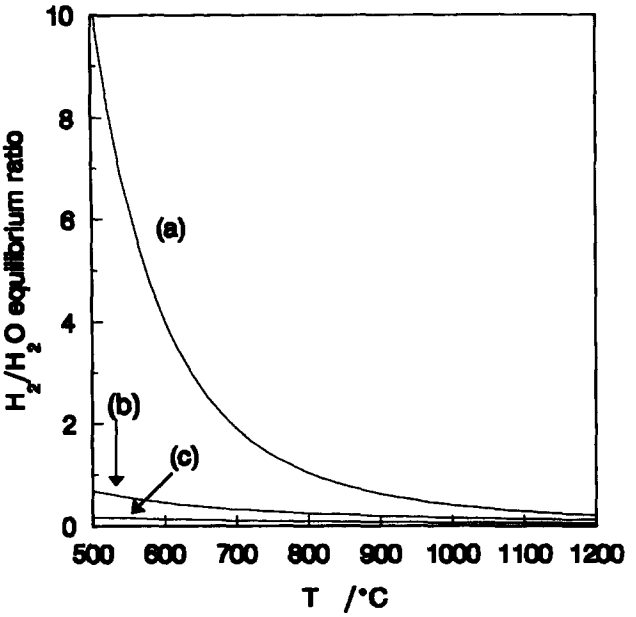

Fig. 4. The H_2/H_2O equilibrium ratios for the reduction of (a) WO_2 to tungsten metal, (b) $W_{18}O_{49}$ to WO_2, and (c) $W_{20}O_{58}$ to WO_2.

and mass-transfer plays an important part in the reduction at the temperatures and flow-rates investigated. Samples interrupted during reduction were often different colours at the front and at the back of the boat. The more reduced phase was always found towards the end of the boat facing the incoming hydrogen stream, which is the more reducing end of the boat. These observations are additional evidence for a mass-transfer-controlled process.

The TCD system could not be operated at high flow-rates, so the kinetics of the system in the regime where the reaction is not controlled by mass-transfer could not be investigated.

3.1.1. Morphological changes

The changes in the morphology of WO_3, heated at 875°C in hydrogen flowing at 200 mL min^{-1}, were studied at different times during the reduction. The original particles were uncharged after 1.5 min, at which stage the sample was almost entirely $W_{20}O_{58}$. Small textured patches were observed on the surfaces and may indicate nucleation of $W_{18}O_{49}$, the next phase to be formed.

After 2.5 min, the surfaces of the original particles were covered in a network of thin needle-like crystallites, which were randomly oriented in the plane of the pseudomorph's surface. This network was little changed after reduction for 3.5 min. Rounded mounds of coral-like clusters were observed in a sample reduced for 5 min, Fig. 5(a); these are probably clusters of WO_2, which was the main constituent of the sample.

After 12 and 16 min, the morphology of the particles had changed significantly. Many psedumorphs of the starting WO_3 particles had broken into smaller agglomerates. These agglomerates were composed of approximately spherical, multi-facetted particles of differing sizes among which coral-like clusters were scattered, Fig. 5(b). Growth ledges were apparent on some of the particles and are indicative of gas-phase

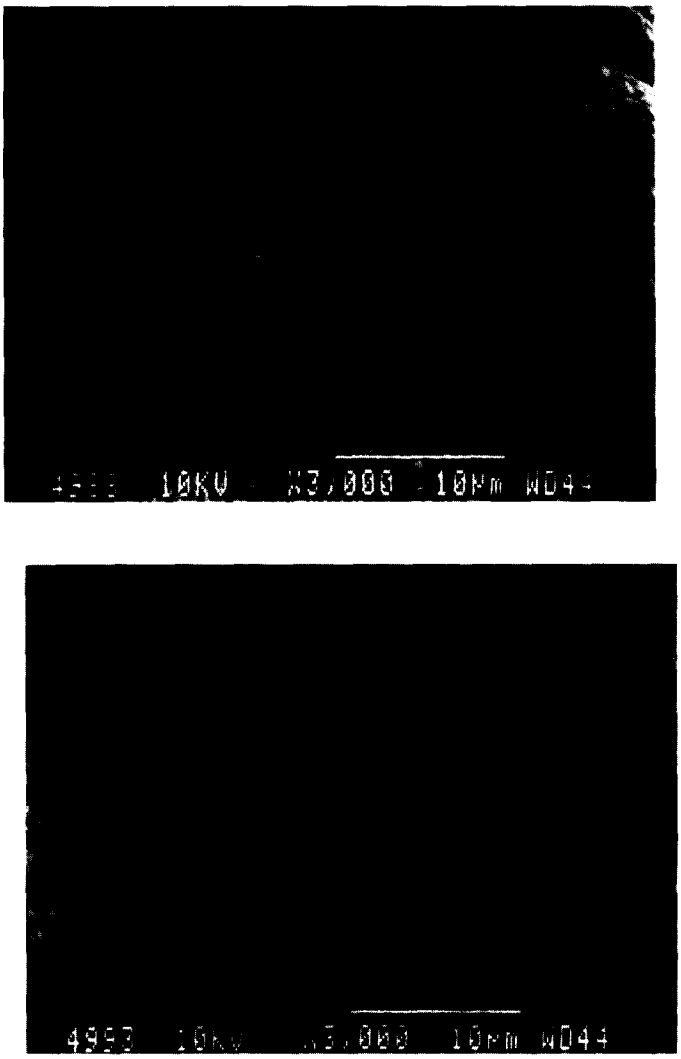

Fig. 5. Scanning electron micrographs of WO_3 reduced in hydrogen (200 mL min^{-1}) at different temperatures and times: (a) 5 min at 875°C; (b) 12 min at 875°C; (c) 2.5 min at 975°C; (d) product under dry conditions at 875°C (0.25 g WO_3, 400 mL min^{-1} H_2); (e) product under normal conditions at 875°C (1.2 g WO_3, 200 mL min^{-1} H_2).

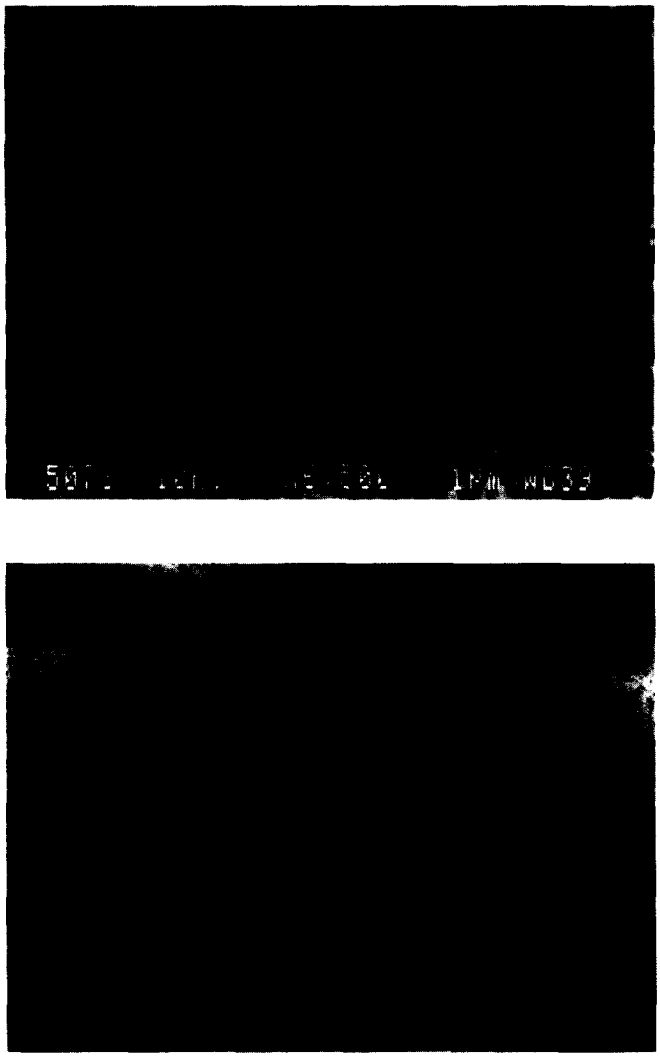

Fig. 5. (*Continued*).

crystal formation [11,12]. The spherical particles are probably tungsten, which was the major constituent of the sample [12,13]. The coral-like clusters are probably WO_2, which was present in the sample in lesser quantitites.

At low temperatures (575 and 675°C) the shapes of the original WO_3 particles were retained by the start of the last stage of reduction, but they had become more porous with star-shaped cracks apparent. At 775°C and above, particles were more rounded and sintered to form quite dense clusters (Fig. 5(a)). The shapes of the pseudomorphs

(e)

Fig. 5. (*Continued*).

lost much of their definition and also increased in porosity. The rounding of the WO_2 particles indicates increased mobility of the tungsten and oxygen atoms, perhaps through the gas phase (via $WO_2(OH)_2(g)$ or gaseous tungsten oxides), or by surface diffusion.

The hydrogen flow-rate and the sample size exerted a large influence on the morphology, through their effects on the partial pressure of water vapour in the powder. In very dry conditions (400 mL H_2 min^{-1} and 0.25 g WO_3) needles were still evident by the time the sample was mainly WO_2, at which stage the pseudomorphs were only slightly porous. The pseudomorphs increased in porosity in more humid conditions and became quite rounded. The sizes of the tungsten crystals were larger when the conditions were more humid. In very dry conditions there were no distinct tungsten single crystals as were observed under other conditions.

At 975°C and 200 mL H_2 min^{-1}, a number of dense clusters of rounded particles were observed in the needle network, which is consistent with the formation of WO_2 from $W_{18}O_{49}$ (Fig. 5(c)). The rounded shapes of the WO_2 clusters contrast with the well-defined needles of $W_{18}O_{49}$, again suggesting that WO_2 has relatively high mobility. Textured patches similar to those observed at 875°C were also apparent at 675°C, which also suggested the formation of $W_{18}O_{49}$ on the surface of $W_{20}O_{58}$ particles.

The size and shape of the final products of the reduction varied considerably under different experimental conditions. At 875°C in very dry conditions, the pseudomorphs

were composed of very small crystals of tungsten, usually less than 0.5 μm in diameter (Fig. 5(d)). More humid conditions resulted in the formation of larger tungsten crystals in open skeletal networks (Fig. 5(e)).

3.2. *Reduction of tungsten oxides with carbon and hydrogen*

The simultaneous use of the graphite and hydrogen in the reduction of WO_3 was studied in the tube furnace, under similar conditions to the reductions when only one reducing agent was used. Sample masses used were 1.2 to 1.3 g, a flow-rate of 200 ml min^{-1} and the stoichiometric ratio was 1 mol WO_3 to 4 mol graphite. WO_3-graphite mixtures had about a 13% larger volume than the equivalent mass of WO_3, but contained only 83% WO_3 by mass. These differences have opposite effects: smaller amounts of WO_3 produce less water vapour, which leads to a higher H_2/H_2O ratio in the powder layer; while a larger volume of powder decreases the rate at which H_2 diffuses in the powder, thus lowering the H_2/H_2O ratio.

The reduction of WO_3–graphite mixtures by hydrogen at 675°C was virtually identical to the reduction of WO_3 by hydrogen alone, as would be expected from thermodynamic and kinetic considerations. At 775°C, however, the graphite-containing mixtures (Fig. 6) were reduced considerably more rapidly than WO_3 alone (Fig. 2). The traces of the CO_2 and CO concentrations showed that these gases were only evolved in noticeable quantities during the first two stages of the reduction. At 875 and 975°C, similar features to the reduction at 775°C were observed, as well as a significant increase in the CO concentration towards the end of the reduction (Figs. 7 and 8). The transition from the third to the fourth stage was also more marked in the TCD trace than when graphite was not present.

The CO_2 concentration increased sharply and briefly at the beginning of the reduction. After reaching a minimum at the transition from the third to the fourth stages of the reduction, the concentration increased slowly and reached a small second maximum at the same time as the CO concentration reached its maximum. The concentration of CO_2 evolved from the sample is thus only appreciable at the start of the reduction and probably does not result from the reduction of WO_3 with CO, since the concentration of CO in the sample is very low initially. The CO_2 is also not likely to be formed by the reduction of water vapour:

$$C + 2H_2O \rightarrow CO_2 + 2H_2 \text{ or } CO + H_2O \rightarrow CO_2 + H_2$$

because the water vapour concentration is reasonably high throughout the reduction process, which implies that the concentration of CO_2 should also be significant throughout the process.

A more likely explanation for the formation of CO_2 is that WO_3 dissociates at high temperatures, and the oxygen from the dissociation reacts with carbon to form CO_2. Another possibility is that the CO_2 is formed from reaction at the points of contact between the WO_3 and the graphite particles. The duration of the first peak in the reduction of WO_3 with graphite (in the absence of hydrogen) was of approximately the same duration as when the reduction took place in hydrogen, which suggests that CO_2

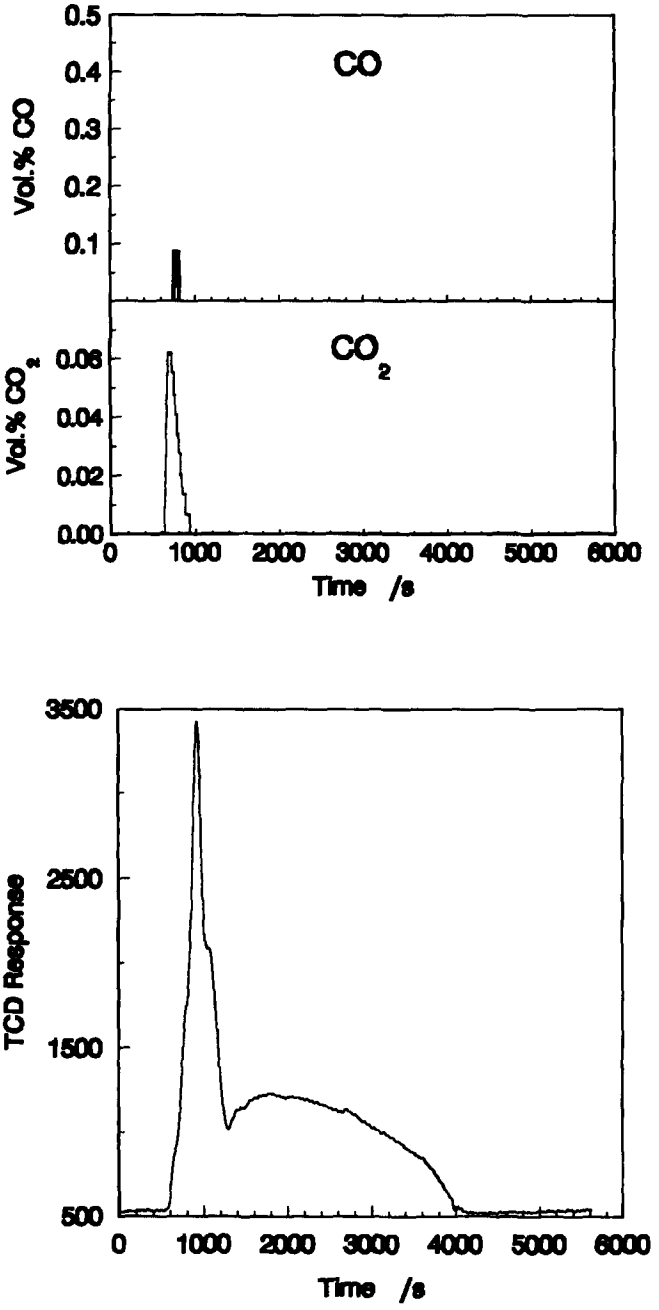

Fig. 6. The concentration of evolved gases during the reaction of WO_3–graphite mixtures (in a 1 : 4 mol ratio) with hydrogen (200 mL min^{-1}) at 775°C.

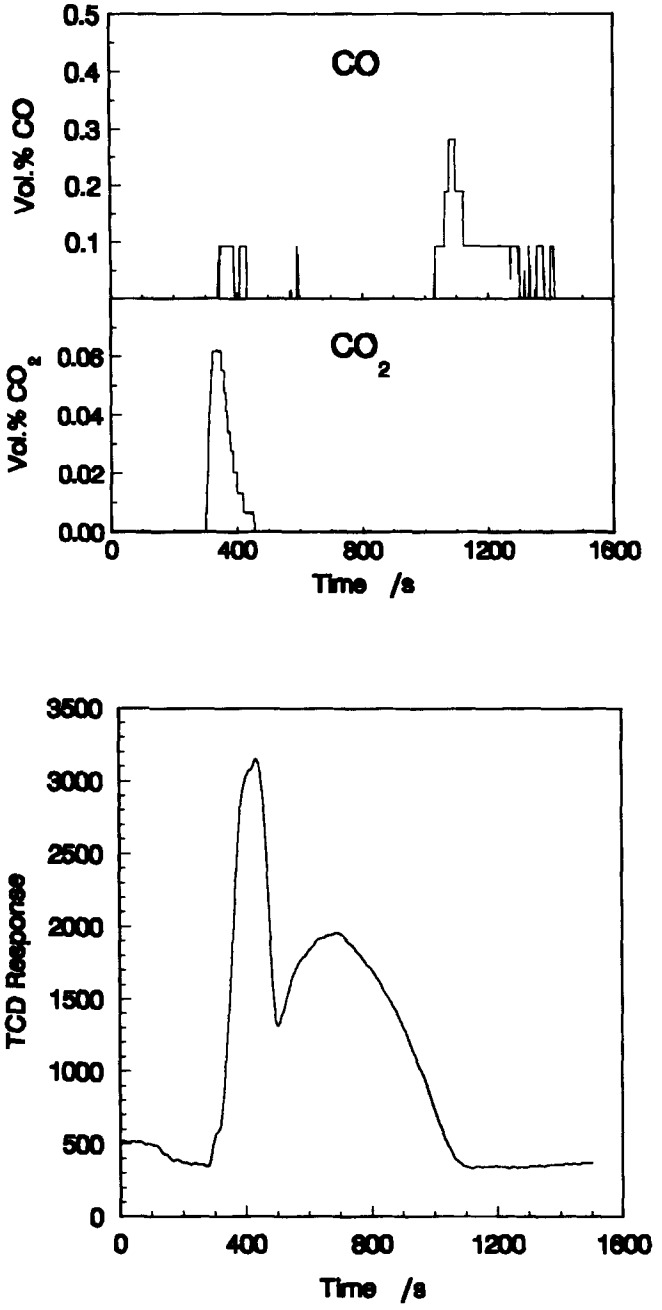

Fig. 7. The concentration of evolved gases during the reaction of WO_3–graphite mixtures (in a 1:4 mol ratio) with hydrogen (200 mL min^{-1}) at 875°C.

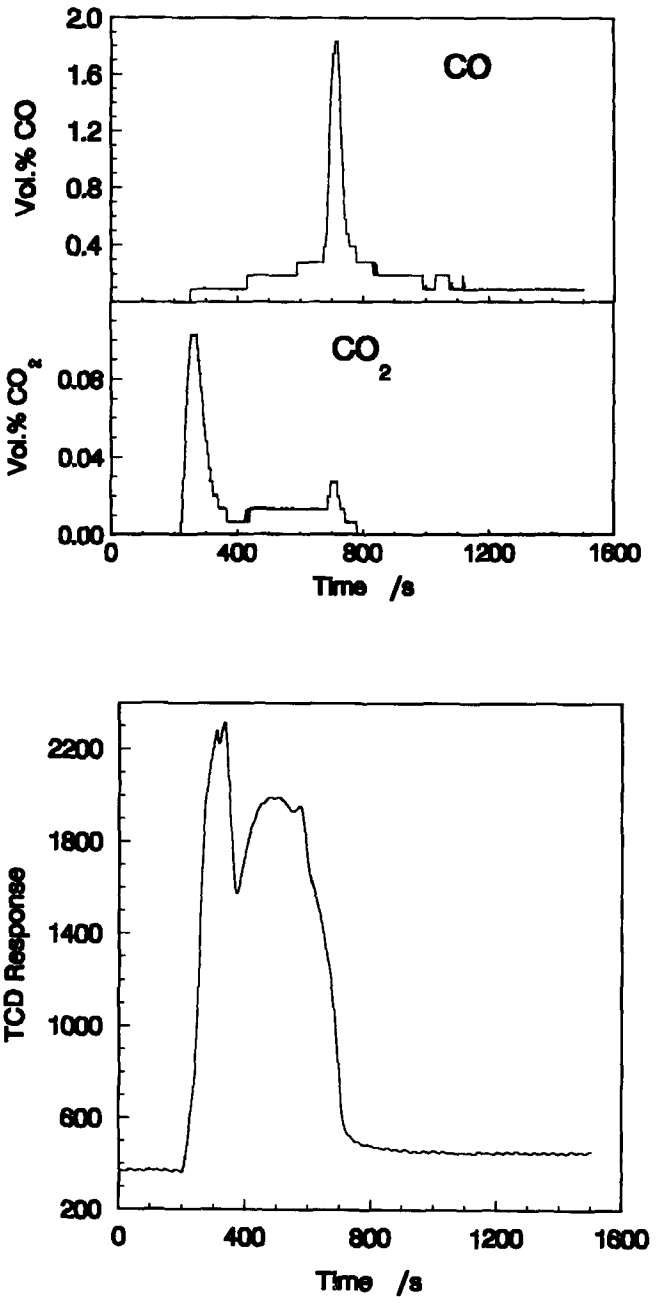

Fig. 8. The concentrations of evolved gases during the reaction of WO_3–graphite mixtures (in a 1:4 mol ratio) with hydrogen (200 mL min^{-1}) at 975°C.

results from the interaction of WO_3 and carbon, and does not involve participation by hydrogen or water vapour.

The peak in the CO concentration at the end of the reduction process is not so readily explained. The reaction of water vapour with CO is expected to be appreciable. If CO is evolved in reasonable quantities throughout the reduction then it must be retained in the sample, and released only at the end of the reduction. CO may be retained in the sample either by adsorption or by reaction to form a carbide. If CO is adsorbed, then the evolution of CO at the end of the process might result from the change in the H_2/H_2O ratio facilitating the desorption of CO from the tungsten surface. Alternatively, if CO reacts to form a carbide, then towards the end of the process the surface of all the freshly generated tungsten may have reacted with CO to form a carbide. If this occurs, further reaction of CO with tungsten would have to take place across a protective layer of carbide and would occur slowly. Thus, the remaining CO in the system would not be consumed as rapidly and would be removed in greater quantities from the powder layer.

The product of the reduction of WO_3–graphite mixtures at 875 and 975°C was predominantly α-W with small amounts of W_2C.

The durations of the first to the third, and of the fourth stages in WO_3–graphite mixtures are compared with the duration of these stages in the absence of graphite in Table 1. The relative increase in the reaction rates is quite similar for the first to the third, and for the fourth stages of the process, Table 4.

The composition of the sample at different times in the reduction was analysed for 1:4 mol ratios WO_3–graphite mixtures at 875 and 975°C in hydrogen flowing at 200 mL min^{-1}. The results are presented in Table 5. The reaction paths are the same as in the absence of graphite, but may also include the reduction of $W_{20}O_{58}$ to WO_2. No W_2C was observed during these experiments and is probably only formed right at the end of the reduction, when the CO concentration is highest.

As in the absence of graphite, the flow-rate had a considerable influence on the rate of reduction. Table 6 lists the duration of the first to the third, and of the fourth stages of the reduction for different flowrates. The fourth stage of the reaction is more affected by the flow-rate than the preceding stages, as is expected from the higher H_2/H_2O equilibrium ratio (Fig. 4). In samples interrupted during the course of the reduction, the

Table 4
The durations of the first three stages, and of the fourth stage, of reaction, for the reaction of WO_3–graphite mixtures in hydrogen. The relative duration of these stages to the corresponding stages in the absence of graphite are also reported

Temp/°C	Duration of Stages 1–3/s	Duration relative to absence of graphite/%	Duration of Stage 4/s	Duration relative to absence of graphite/%
775	355	72	1346	75
875	181	62	586	62
	216	74	622	66
975	176	70	345	70
	181	72	415	85

Table 5
Composition of WO_3–graphite mixtures after reduction in hydrogen (200 mL min^{-1}) at 875 and 975°C

Time/s	Mass loss/%	Phase identified besides graphite
875°C		
1	0.71	WO_3
2	2.33	$W_{20}O_{58}$; WO_2; small amounts $W_{18}O_{49}$
3.5	4.15	WO_2; $W_{18}O_{49}$
6	9.12	Mostly WO_2; some α-W
10	15.17	Mostly α-W; some WO_2
975°C		
2	4.59	Mostly WO_2; some $W_{18}O_{49}$
5	11.12	α-W; WO_2

Table 6
Effect of the hydrogen flow-rate on the durations of the first to the third stages, and of the fourth stage of the reduction of a 1:4 mol ratio WO_3–graphite mixture

Temperature/°C	Flow-rate/(mL min^{-1})	Duration	
		Stages 1–3/s	Stage 4/s
875	200	216	586
		216	622
	400	207	425
975	200	176	345
		181	415
	400	150	252

colour of the sample often varied across the length of the boat. These observations again indicate that reaction was limited by mass-transfer.

The effect of varying the amount of graphite in the system was studied by examining the reductions of WO_3–graphite mixtures in 1:2 and 1:8 mol ratios. The mixtures examined were the same mass as used previously (i.e., 1.2 g). The mass of WO_3 in the sample is likely to affect the rate of the reduction because more water vapour will be formed when the sample contains larger amounts of WO_3. This will lower the H_2/H_2O ratio, and hence may decrease the rate of reduction. The durations of stages one to three, and of stage four of the process as a function of the WO_3 mass in the sample are shown in Fig. 9 for reaction at 875°C. The durations of the stages are also shown for a 0.5 g sample of WO_3.

The durations of the first three stages of reaction were noticeably shortened by the presence of graphite. Increasing the proportion of graphite in the sample did not have

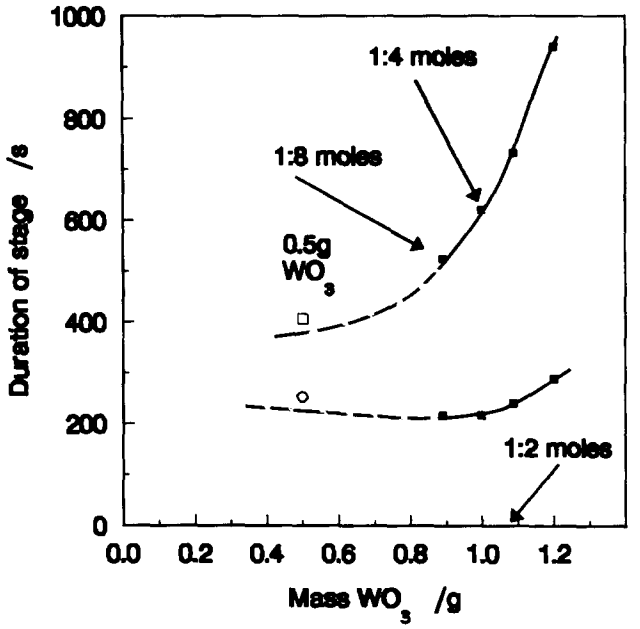

Fig. 9. The effect of the mass of WO_3 in a WO_3–graphite mixture on the duration of the first three stages, and of the fourth stage. The points at 0.5 and at 1.2 g correspond to samples containing WO_3 only.

much effect above a 1:4 mol ratio. The duration of the same stage, for a 0.5 g sample of WO_3, was longer than that of the mixtures, which proves that decreasing the WO_3 mass in the sample at different mixtures was not solely responsible for the increased rate of reduction, and that graphite increased the rate of reduction.

The fourth stage of the process was considerably shorter when graphite was present, but the effect might also be caused by the associated decrease in the WO_3 mass of the sample as the stoichiometric ratio increases. For example, the duration of the fourth stage in the reduction of 0.5 g of WO_3 was similar to that obtained by extrapolating the curves of WO_3–graphite mixtures to the composition which would correspond to 0.5 g of WO_3, in a 1.2 g WO_3–graphite mixture. The stoichiometric ratio of WO_3 to graphite in a 1.2 g mixture which contained 0.5 g WO_3 would be 1:27, which corresponds to a 1:4.4 volume ratio. This increase in the volume of the mixture is likely to decrease the rate of transport of hydrogen through the powder layer, which would attenuate the observed effect of graphite on the duration of the fourth stage. Therefore, the fourth stage is probably accelerated by graphite, but this assertion could not be definitely proved without a more detailed knowledge of the effective diffusivities in the system and how they affect the reduction rate.

The amount of graphite which reacted during the process was taken as the difference between the mass loss from the sample and the theoretical mass of oxygen in the sample. Results are listed in Table 7 for reactions under different conditions. These

Table 7
The percentage mass of graphite reacted during the reduction of WO_3–graphite mixtures with hydrogen

Temperature/°C	Flow-rate/(mL min^{-1})	Stoich. ratio	Mass loss/%
775	200	1:4	0.6
875	200	1:4	1.3
	400	1:4	0.9
	200	1:2	0.4
	200	1:8	0.6
975	200	1:4	1.1
			1.1
	400	1:4	1.1

results show a reasonably consistent increase in the amount of graphite reacted as the temperature and stoichiometric ratio of the mixtures are increased.

3.2.1. Morphological changes

The appearence of WO_3–graphite mixtures was relatively unchanged after heating in the furnace for 1 min at 875°C in a flow-rate of 200 mL H_2 min^{-1}, although patches of the WO_3 surface had started to become textured. Needle-like crystallites were visible after 2 min, but were much less extensive than in the absence of graphite, and were interspersed between relatively smooth round regions of up to 3 μm in diameter (Fig. 10(a)). These round patches (which were often cracked in the centre) were probably the WO_2 which was present in the sample. After 3.5 min, the needles were longer and covered a larger proportion on the surface.

The less extensive formation of needles of $W_{18}O_{49}$ when graphite was present probably indicates that the water vapour concentration in the system was lower. Similar morphologies were seen when the flow-rate was decreased, and Schubert [9] has also observed the reduction of $W_{20}O_{58}$ to WO_2 in dry conditions.

Reduction for 6 min resulted in the disintegration of needles to form small particles which were sometimes clustered into mounds. The surfaces of pseudomorphs after reduction for 10 min were quite similar, although the growth of crystals with clear facets was observed in cracks. Patches of small elongated tungsten or tungsten oxide particles were often observed on the surface of the graphite particles. These observations are similar to those for the reduction of WO_3 in the absence of graphite.

At 975°C, the morphologies of tungsten oxide particles at different times during the reduction were similar to those observed at 875°C. Small nodules of tungsten or tungsten oxides were seen on the graphite particles. Increasing the stoichiometry did not have much effect on the morphology of the tungsten oxide particles.

At the end of the process, the tungsten particles were collected in loose, open networks. Small graphite particles were sometimes incorporated on the surface of these structures. Tungsten nodules were often observed on the surfaces of the graphite particles (Fig. 10(b)). The tungsten particles were up to 2 μm in diameter at 875°C (Fig. 10(c)). Similar morphologies were observed at 975°C.

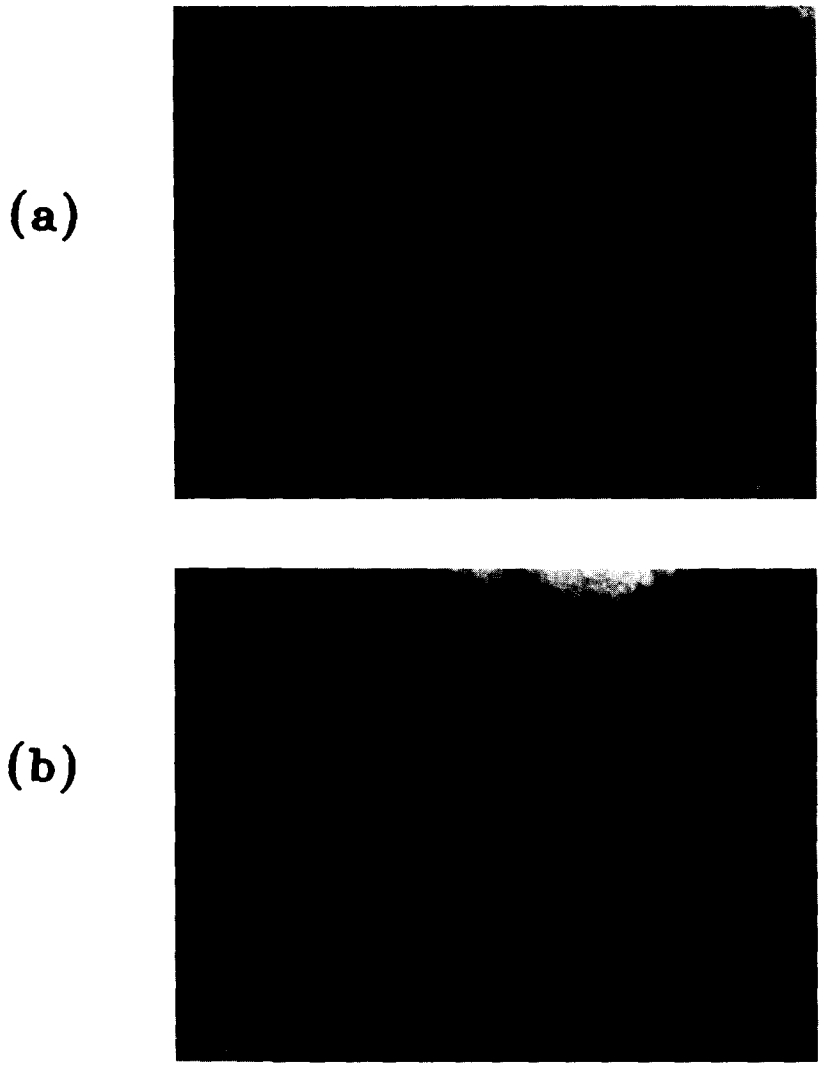

Fig. 10. Scanning electron micrographs of the reaction of WO_3–graphite mixtures (1:4 mol ratio) in hydrogen at different times and temperatures: (a) 2 min at 875°C; (b) and (c) products at 875°C.

4. Conclusions

The reduction of tungsten oxides with hydrogen and the reaction of mixtures of tungsten trioxide and carbon with hydrogen have been studied. These results may be compared with similar studies of reduction with carbon alone [6,7] and with carbon monoxide [8]. The kinetics and mechanisms of these reductions under the conditions investigated are summarised in Table 8.

(c)

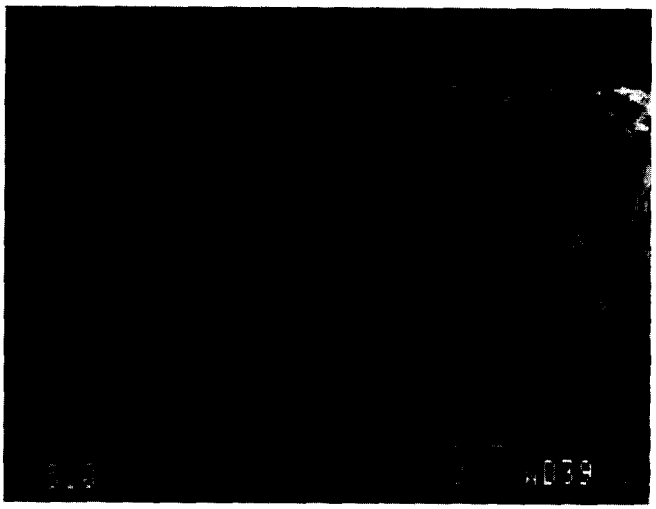

Fig. 10. (*Continued*).

Table 8
The kinetic models which best described the reactions investigated, and the activation energies, E_a, calculated for the reactions

System	Conditions	Kinetic model	E_a/(kJ mol^{-1})
WO_3–CO	First stage	Zero-order R2	66 ± 2
	Second stage	Zero-order	33 ± 8
WO_2–CO		R2	62 ± 5
WO_3–C	TG, graphite, first stage	D4	389 ± 9
	second stage	F1	438
	TG, lamp black, first stage	D4	465
	Tube furnace, graphite, first stage	D4	374 ± 2
WO_3–H_2	Mass-transfer controlled	–	–
WO_3–C–H_2	Mass-transfer controlled	–	–

The reduction of WO_3 with carbon takes place above 900°C via the formation of CO, and involves two distinct stages. The rate of the first stage was proposed to be limited by diffusion. Activation energies of 386 ± 9 kJ mol^{-1} and 465 kJ mol^{-1} were calculated from TG experiments [6] for the reduction with graphite and lamp black, respectively. From data obtained from the tube furnace experiments [7], an activation energy of 374 ± 2 kJ mol^{-1} was calculated for the reduction with graphite. The rate of the second stage was proposed to be limited by the rate of the reaction of CO_2 with graphite.The activation energy for this stage was 438 kJ mol^{-1}. The importance of the CO/CO_2 ratio in the system, and its effect on the reaction rate of CO_2 with carbon, were related to the observed change in the kinetic obedience of the system [6,7].

The reactions of WO_3 and WO_2 with CO [8] to form WC were examined from 650 to 900°C. The reduction of WO_3 occured in two distinct stages below 800°C. The first-stage of the reaction was proposed to be related to the reduction of WO_3 to $W_{20}O_{58}$ and some $W_{18}O_{49}$. The activation energy was 66 ± 2 kJ mol^{-1}. Further steps resulted in the formation of $W_{20}O_{58}$, $W_{18}O_{49}$, and WO_2. The rate of the main part of the reduction was phase-boundary controlled with an activation energy of 40 ± 7 kJ mol^{-1}.

The reduction of WO_2 also occurred in a single stage, and was best described by the R2 model. An activation energy of 62 ± 5 kJ mol^{-1} was calculated. The reduction was preceded by a short induction period, possibly signifying the formation and growth of nuclei.

Differences between the kinetics of the reductions of WO_3 and WO_2 with CO, and the reduction of WO_3 with carbon, were explained in terms of different CO/CO_2 ratios in the powder layer.

The experimental arrangement was such that the kinetics of the reductions of WO_3 with hydrogen, and with carbon and hydrogen, could not be studied outside a mass-transfer-controlled regime. Regardless of whether or not carbon is present, the reduction of WO_3 with hydrogen is rapid and the H_2/H_2O ratio in the powder layer soon approaches the equilibrium ratio for the reaction taking place. The usual technique of studying the kinetics of the reaction by decreasing the temperature until mass-transfer is no longer rate-limiting could not be applied in this system owing to the substantial increase in the H_2/H_2O equilibrium ratio at lower temperatures.

The presence of graphite increased the rate of reduction of WO_3 with hydrogen above 675°C. The overall effect of graphite seems to be to decrease the amount of water vapour in the system, thus leading to an increased reaction rate. The rate of the final stage of the reduction also appeared to increase in the presence of carbon. This effect could not be proved conclusively because the effect of a decreased proportion of WO_3 in the sample, and changes in the porosity and effective diffusivities of the WO_3–graphite mixtures, were not fully known.

Evolved gas analysis showed that significant amounts of CO_2 were evolved during the initial stages of the reduction, after which the concentration of CO_2 in the system was very low. The concentration of CO evolved from the system increased only at the end of the reduction. The amount of CO evolved at this stage of reaction increased markedly with temperature.

Acknowledgements

The authors acknowledge with gratitude the advice and assistance given by Karol Cameron, Ian Sutherland and Ian Poree of the Solid State Chemistry Group, AECI Chemicals Ltd, and financial support from AECI Chemicals Ltd and the Foundation for Research Development.

References

[1] J.A. Mullendore, in Kirk–Othmer Encyclopedia of Chemical Technology, 3rd edn., Vol. 23, John Wiley and Sons, New York, 1983, pp. 413ff.

[2] T. Millner and J. Neugebauer, Nature (London), 163 (1949) 601.
[3] W.D. Schubert and E. Lassner, Int. J. Ref. Hard Met., 10 (1991) 171.
[4] W.D. Schubert and E. Lassner, Int. J. Ref. Hard Met., 10 (1991) 133.
[5] A.S. Petukhov, L.D. Konchakovskaya, I.V. Uvarova and L.G. Reiter, Poroshk. Metall. (Kiev), (6) (1990) 33 (Chem. Abstr., 114 (1990) 10482v).
[6] D.S. Venables and M.E. Brown, Thermochim. Acta, 282/283 (1996) 251.
[7] D.S. Venables and M.E. Brown, Thermochim. Acta, 282/283 (1996) 265.
[8] D.S. Venables and M.E. Brown, Thermochim. Acta, accepted for publication.
[9] W.D. Schubert, Int. J. Ref. Hard Met., 9 (1990) 178.
[10] J. Szekely, J.W. Evans and H.Y. Sohn, Gas–Solid Reactions, Academic Press, London, 1976.
[11] P. Taskinen and M.H. Tikkanen, Scand. J. Metall., 6 (1977) 223.
[12] R. Haubner, W.D. Schubert, E. Lassner, M. Schreiner and B. Lux, Int. J. Ref. Hard Met., 2 (1983) 108.
[13] R. Haubner, W.D. Schubert, H. Hellmer, E. Lassner and B. Lux, Int. J. Ref. Hard Met., 2 (1983) 156.